Biomedical engineering

# Quantitative assessment of the static properties of the oculo-motor system by the photo-oculographic technique

C. Buquet J.R. Charlier

Institut National de la Santé et de la Recherche Médicale, Unité 279, Lille, France

**Abstract**—*The paper addresses the problems raised by the application of the photo-oculographic technique to the quantification of static orientations of the eye in ophthalmology. Eye orientations are determined from the relative positions of corneal reflex and pupil images. The relationship between the positions of these images and the angular rotations of the eye is studied with an optical model of the anterior chamber of the eye. This model is used to analyse the influence of technical and physiological variables and to evaluate the accuracy of different calibration procedures applicable to clinics.*

**Keywords**—*Eye movements, Image analysis, Ophthalmology, Strabismus*

Med. & Biol. Eng. & Comput., 1994, 32, 197–204

## 1 Introduction

Abnormalities of ocular motility are often the clue to the localization of a central or peripheral disease of the visual sensory motor system. Their evaluation can contribute significantly to diagnostic and therapeutic decisions made by clinicians. However, the various methods available in the clinic environment present important limitations. Direct viewing of the subject's eyes allows at most a precision of 2° and does not provide objective documentation. With the electro-oculographic technique (Marg, 1951; Reinecke, 1961*a*; *b*), drifts of the electrode potential do not allow absolute measurements, and heterogeneities of the bio-electric field considerably reduce the reliability of measurements along the vertical and oblique axes (Zao *et al.*, 1952; Quere *et al.*, 1973; Buquet *et al.*, 1989*a*). With the magnetic-coils technique (Robinson, 1963), the use of scleral lenses makes the examination difficult with children and unco-operative patients. With the limbus reflectance technique (Torok *et al.*, 1951; Smith and Warter, 1960; Gauthier and Volle, 1975; Reulen *et al.*, 1988), measurements are unreliable along the vertical and oblique axes owing to the masking of the iris margin by the eyelids. With the methods based on the first and fourth Purkinje images (Crane and Steele, 1978; Barry *et al.*, 1992), the range of measurements is limited as the reflection of a light source over the back of the lens is only visible for small deviation angles.

The photo-oculographic (POG) technique is an attractive solution to these problems. It is based on the measurement of the position of the corneal reflex relative to the pupil (Hirschberg, 1885), which is directly related to the gaze direction by the geometry of the eye anterior chamber. It allows an isotrope and stable evaluation of the angular eye rotation and is not sensitive to translation movements of the head. Technological developments of video sensors, electronics and microprocessors have permitted the automated analysis of these eye images and opened the way to the realisation of objective recordings based on the Hirschberg principle (Merchant *et al.*, 1974; Fourcy *et al.*, 1980; Charlier and Hache, 1982; Barbur *et al.*, 1987).

However, applications of the POG technique to the clinic have been confronted by many problems. Variations of pupil size or eye fundus reflectance result in changes of the image contrast and produce recording artefacts when the detection of the pupil contour and of the corneal reflex is made by thresholding the video signal, as in the studies mentioned previously. Other sources of error involve the partial masking of the pupil by eyelids or eyelashes and parasitic light reflections. These problems have been solved by applying automated pattern-recognition techniques to the detection of the pupil contour and of the corneal reflex image (Charlier *et al.*, 1985; Buquet *et al.*, 1988).

Clinical evaluations have demonstrated the significant improvements brought about by these techniques in the evaluation of vertical and oblique movements (Quere *et al.*, 1990*a*) and of vergence (Quere *et al.*, 1990*b*; *c*). These preliminary evaluations have raised new equations regarding the clinical applications and limitations of the POG technique.

This paper presents methodological and technical developments that have been made to provide solutions to these questions. First, there is the need for quantification of results. For the diagnostic of alterations, the results from one patient must be compared with references from a normal population, and the results from the pathologic eye of a patient must be compared with those of the other, normal, eye. Follow-up treatment requires the comparative analysis of the results from a series of examinations.

*First received 2 October 1992 and in final form 25 February 1993*

After a short reminder of the main features of the POG technique, this paper addresses the question of how the needs for a quantitative evaluation can be met for the static characteristics of the oculo-motor system.

## 2 Background

The main features of the POG technique have been described previously (CHARLIER and HACHE, 1982; CHARLIER *et al.*, 1985; BUQUET *et al.*, 1988). The subject's eye is illuminated with near infra-red radiation (880 nm). The first part of the incident light rays is reflected by the front of the cornea and produces the so-called corneal reflection.

The other part of the incident light is reflected from the retina and back-lights the pupil. A standard 525 interlaced scanning lines, 60 frames per second, charge coupled device (CCD) camera is used as an image transducer. The sensor covers a 15 mm × 15 mm image area of the eye, with a resolution of 256 lines of 256 pixels each. The resulting video signal is processed to determine the relative positions of the corneal reflex and pupil images. Experience has shown that simple threshold methods are not reliable for the detection of these images. Large variations of luminance levels result from changes in pupil size and eye fundus reflectance. Furthermore, artefacts such as partial masking of the pupil by eyelashes or eyelids and parasitic reflections are encountered in a large number of subjects. The need for an automated analysis of these images has led to the use of automated pattern-recognition techniques.

In the first step, the leading and trailing edges of the pupil contour and the spike formed by the corneal reflex are detected from the video signal by dedicated hardware circuitry using specific shape discrimination (CHARLIER *et al.*, 1985) (Fig. 1). The horizontal and vertical co-ordinates of these three types of event are digitised and transmitted to corresponding digital memories.

In the second step, a ZILOG 80280 microprocessor classifies these events in order to eliminate those produced by artefacts. These classifications rely on the relative spatial arrangement of events. The pupil contour is easily identified by its characteristic oval shape. For the corneal reflex, a specific pattern of five individual light sources is used to obtain a reliable identification.

In the last step, the microprocessor determines the centre of the corneal reflex pattern and of the pupil by applying best-fitting algorithms to the sets of validated events. Additional parameters are also calculated that provide additional information on the reliability of the image analysis. These parameters include the radii of the pupil and of the corneal reflex pattern and the number of events used for the determination of the pupil and corneal reflex. These calculations are performed in real time (60 Hz), and their results are output to the main microcomputer via an RS232 interface.

## 3 Methodology

The evaluation of the static characteristics of the oculo-motor system requires a precise determination of the relative orientations of the visual axis of both eyes and of the direction of a visual stimulus used to elicit eye fixations or movements (Fig. 2). The orientations of the visual axis are related to the positions of the images of the pupil and corneal reflex through physiological parameters that characterise the biometry of the anterior chamber of the eye. The relationship between the position of these images and the measured data involves technical parameters. A precise knowledge of these physiological and technical properties is important for the determination of calibration procedures and for the interpretation of results.

The precision of spatial measurements relies on the absolute precision of the two eye movement sensors and of the visual stimulus generator.

A rigid mechanical bench has been designed to assure a precisely defined and reproducible mechanical position of these elements (Fig. 3). This bench includes adjustments for the position of each eye movement sensor along the horizontal, vertical and depth axes, allowing adaptation to the head morphology of individual subjects.

Many solutions have been proposed for the generation of visual stimuli for eye movement studies. The projection of a light beam deviated by two mirrors (QUERE *et al.*, 1972; AALTO *et al.*, 1989) is preferable. It offers more flexibility than linear arrays of light-emitting diodes (JANTTI *et al.*, 1979), which provide a simple and inexpensive approach but limit the study of eye movements to one direction at a time.

In our design, the positions of the mirrors are controlled by stepping motors driven by electronic circuitry allowing microsteps of 0·8 arc min and an absolute precision better

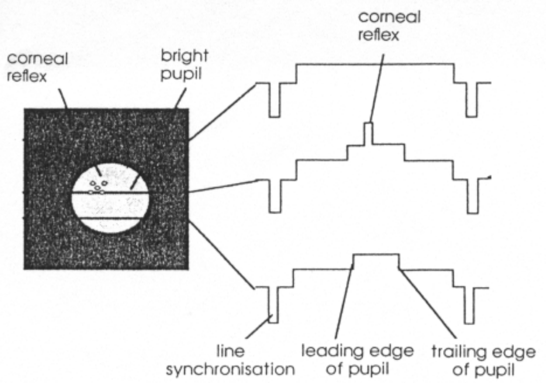


**Fig. 1** *Extraction of the pupil contour and corneal reflex from the video signal*

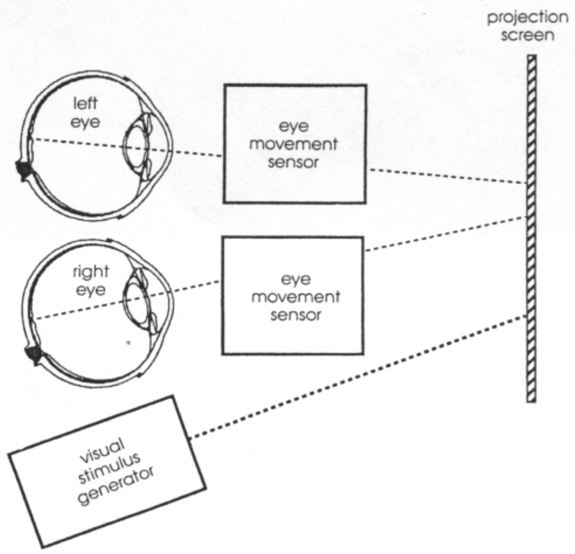


**Fig. 2** *Elements involved in the study of the static oculo-motor co-ordination*

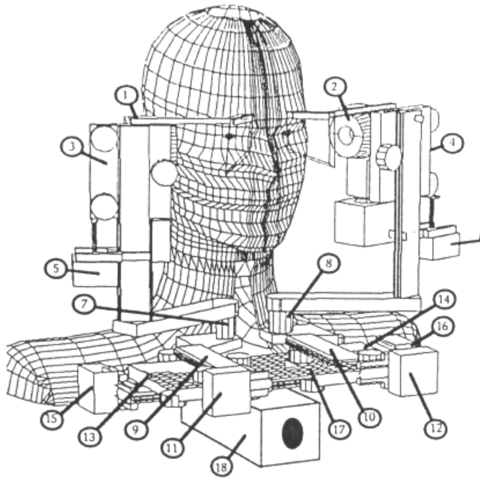

**Fig. 3** *Mechanical stand used for controlling the positions of the two eye movement sensors: 1 and 2 = eye movement sensors; 3 and 4 = carriages for vertical movements; 5 and 6 = linear actuators for vertical movements; 7 and 8 = turrets for rotary motions; 9 and 10 = carriages for movements in depth; 11 and 12 = linear actuators for movements in depth; 13 and 14 = carriages for horizontal movements; 15 and 16 = linear actuators for horizontal movements; 17 = reference bench; 18 = visual stimulator*

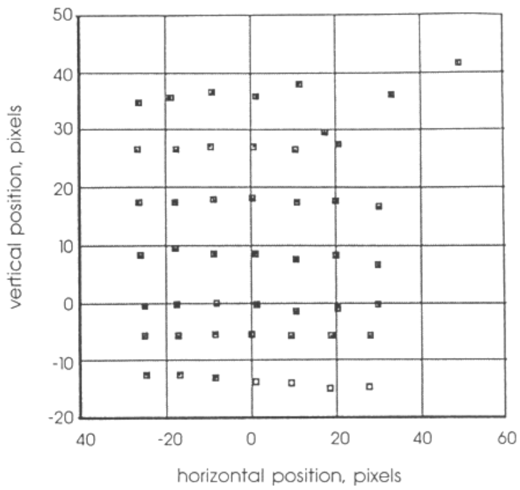


**Fig. 4** *Measurement of the relative position of the pupil and corneal reflex images obtained for a matrix of 49 positions (results from the right eye)*

than 0·2°*. A microprocessor is used to implement algorithms correcting the parallax errors due to the offset of position between the viewing eye and the stimulus generator.

Identical scaling factors of the two eye movement sensors have been obtained by using solid-state image sensors based on charge coupled device (CCD) technology and by specifying the characteristics of their optical elements and image-processing electronics.

## 4 Modelling

### 4.1 *Preliminary evaluation*

A preliminary experimental evaluation has been made to evaluate the relationship between the orientation of the visual axis and the relative positions of the corneal reflex and pupil centre. The positions of the pupil and corneal reflex images have been recorded with the POG technique while the subject fixated monocularly 49 different positions of a red light-emitting diode subtending 8·5 arc min at a viewing distance of 1200 mm. All 49 positions were located in the frontal plane (i.e. the vertical plane perpendicular to the head's median plane), following a 7 × 7 square matrix. The distance between adjacent positions was 140 mm, corresponding to 6·6° of visual angle at the centre of the matrix.

The pupil and corneal reflex images were detected for all 49 positions, except for the three located at the top and on the right side of the matrix (Fig. 4). For these last three positions, the angle between the optical axis of the eye and of the sensor exceeds 35°. This angle is too great to obtain a reflection from the cornea. A reflection is produced over the sclera, but its optical quality is often very poor and does not allow reliable detection. It is relevant to note that the optical axis of the sensor is placed 10° under the horizontal plane in order to reduce artefacts due to the masking of the pupil by eyelashes or eyelids. Furthermore, the optical axis of the eye is about 5° to the temporal side of the gaze direction. With this set-up, the range of the POG technique is limited to gaze angles reaching 25° upward, 45° downward, 40° to the nasal side and 30° to the temporal side.

The results also show evidence of barrel distortion and non-linearities: the lines and columns of the matrix are curved, and the distance between successive lines is not constant. Fitting these data with first-degree linear regression equations results in a mean quadratic error of 2·9°. Furthermore, repeated determinations of the calibration factors show variations leading to errors reaching 3°, indicating that the relationship is influenced by uncontrolled parameters. In order to investigate the origin of these errors, we have developed an optical model of the anterior chamber of the eye and calibration procedures allowing the identification of the parameters of this model.

### 4.2 Model

The gaze direction can be determined from the positions of the corneal reflex and the pupil images through the following equations (Fig. 5) (Young and Sheena, 1975):

$$X_p = (OA - AP')\sin\Theta \quad (1)$$

$$X_c = (OA - AC)\sin\Theta \quad (2)$$

$$X_p - X_c = (AC - AP')\sin\Theta \quad (3)$$

where $\Theta$ is the rotation of the eye; $X_p$ is the position of the centre of the pupil image; $X_c$ is the position of the centre of the corneal reflex pattern; $AP'$ is the distance between the apex of the cornea and the pupil image; $AC$ is the curvature radius of the cornea; and $OA$ is the distance between the apex of the cornea and the centre of rotation of the eye.

The corneal reflex $R'$ is the reflexion of the light source $R$ over the optical diopter formed by the interface between air and the cornea. The image of the pupil $P'$ is obtained by refraction of the real pupil $P$ through the same diopter. The positions of these images are not fixed with respect to the anterior chamber of the eye. They are determined from

* Behague, M.: 'Un nouveau stimulateur pour l'étude des mouvements oculaires.' Personnal communication, 1991.

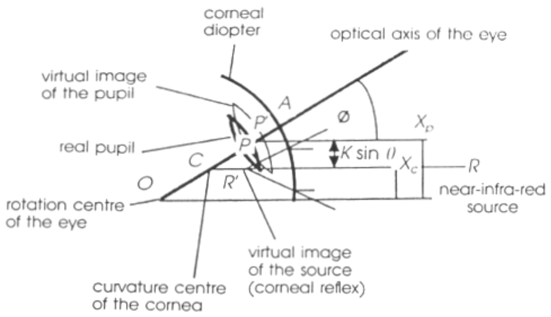


**Fig. 5** *Optical model of the anterior chamber of the eye*

Young's paraxial equations (see Appendix) applied to the light source and to a set of ten points distributed on the pupillary contour (CHARLIER and PARIS, 1987). The centre of the pupil is calculated as the point for which the sum of distances to the equidistant lines of the chords sustained by these ten points is minimum. These equations are solved with a successive numerical approximation technique. The diopter between air and the cornea is supposed to be ellipsoidal, an assumption that can be made for eccentricities up to 30° (DELMARCELLE *et al.*, 1976).

The model takes into account the angle between the optical axis of the sensor and the horizontal plane and the angle between the optical axis of the eye and the gaze direction. It introduces a correction for the parallax error on the position of the corneal reflex. This source of error has already been described previously (BRONSON, 1983): translations of the head produce a small relative displacement of the corneal reflex with respect to the pupil image. With the present optical set-up, a translation of 10 mm results in a relative displacement of 0·4 mm (Fig. 6), which is equivalent to an eye rotation of 5°. This correction factor is not affected by the eccentricity of fixation.

The model introduces another correction for the parallax error on the position of the pupil image. Fig. 7 shows the lateral shift of the pupil image resulting from variations in the pupil size for an average eye (corneal radius = 7·86 mm, depth of the anterior chamber = 3·7 mm, angle of the visual axis relative to the optical axis of the eye = 5°, central fixation). The amount of displacement reaches values equivalent to 1° of eye rotation for a change in pupil radius of 2 mm. It varies with the eccentricity of fixation.

Fig. 8 shows a comparison of the 49 stimulus positions and the corresponding estimations of gaze direction obtained from the previous POG measurements, after application of correction factors determined using the model. These data are both displayed in the referential of the eye image sensor, i.e. with an axis 10° under the horizontal plane. The parameters of the model are determined by minimising the mean quadratic error between the positions of fixation points and the corresponding estimations of gaze direction.

The model corrects the barrel distortion and non-linearities found initially. The mean quadratic error is found to be 0·8° for all 49 points of the matrix, which is to be compared with the 2·9° error found initially. The error is further reduced to 0·7° after exclusion of the three points with the largest eccentricity, and to 0·5° when the model is applied to the points with less than 20° eccentricity.

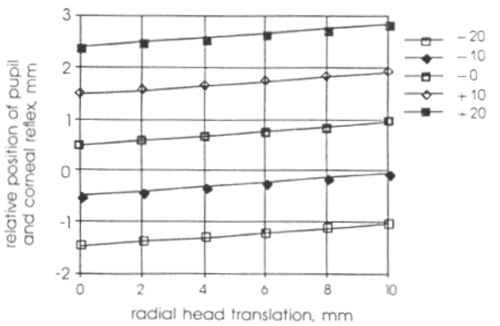


**Fig. 6** *Shift of the position of the corneal reflex relative to the pupil image with head translation calculated from the model for different eccentricities of fixation*

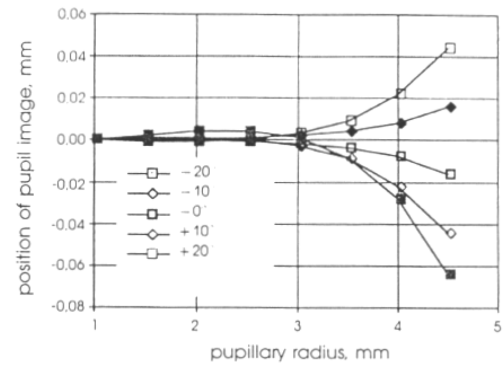


**Fig. 7** *Lateral shift of the position of the pupil image with pupil size calculated from the model for different eccentricities of fixation*

## 5 Application to clinical examinations

### 5.1 *Preliminaries*

The calibration procedure used in the previous paragraph includes 49 calibration points. It is clearly too complicated and time consuming to be applicable to clinical examinations. The identification of the parameters of the model can be facilitated by using additional information about the optical set-up and the biometry of the eye.

The angle between the axis of the optical sensor and the horizontal plane and the distance between the light sources

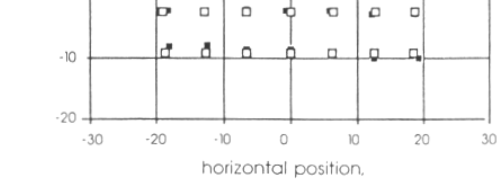


**Fig. 8** *Comparison of the positions of the stimulus (open squares) and of the gaze direction (solid squares)*

and the eye are fixed by the geometry of the optical set-up. The curvature radii of the cornea, the depth of the anterior chamber, the pupil size and the angle between the optical axis and the gaze direction are defined by the geometry of the eye. Some of these parameters can be estimated from the POG measurements: the size of the pupil image is measured directly, and the radius of the cornea can be evaluated from the size of the corneal reflex pattern by applying refraction equations to the air–corneal diopter. Other parameters, such as the depth of the anterior chamber and the angle of the visual axis, can only be estimated through a calibration procedure.

For clinical applications, it is important to know the accuracy of POG measurements obtained after different calibration procedures. With patients who do not co-operate, such as infants, or patients with low vision, calibration cannot even be implemented. For some other patients, calibration can only be made on one eye. With most patients, a calibration with only one point would be easier to perform than one with two or more points.

The accuracy obtained after these various calibration procedures can be inferred from the relative contribution of the physiological parameters to the calibration factors.

### 5.2 *Theoretical approach*

The relationship between the gaze direction, the relative positions of the eye images and the parameters of the model is described by the following equation:

$$X = X[(\Theta - \Theta_0, AC, AP] \qquad (4)$$

with

$$X = X_p - X_c \qquad (5)$$

where $X_p$ is the position of the centre of the pupil image; $X_c$ is the position of the centre of the corneal reflex pattern, $\Theta$ is the rotation of the eye; $\Theta_0$ is the angle of the visual axis with respect to the optical axis of the eye; $AC$ is the curvature radius of the cornea; and $AP$ is the sum of the depth of the anterior chamber and the thickness of the cornea.

In a first approximation, the effects of variations of the biometry can be estimated by derivation of eqn. 4:

$$dK = \frac{\delta K}{\delta AC}\, dAC + \frac{\delta K}{\delta AP}\, dAP \qquad (6)$$

with

$$K = \frac{dX}{d\Theta} \qquad (7)$$

This equation allows the determination of the relative variation of the calibration coefficient $K$ resulting from absolute variations of $AC$ and $AP$ for a given rotation of the eye $(\Theta - \Theta_0)$.

The model allows the calculation of coefficients $\delta K/\delta AC$ and $\delta K/\delta AP$. For the average eye and for a central fixation, the values of these coefficients are found to be $\delta K/\delta AC = 0{\cdot}019^{\circ -1}$, and $\delta K/\delta AP = 0{\cdot}016^{\circ -1}$.

The absolute variations of $AC$ and $AP$ can be determined from biometric data found in the literature. The radius of the cornea averages 7·86 mm, with a standard deviation of 0·26 mm (Cochet *et al.*, 1967). In young subjects, the vertical radius is, on average, 0·16 mm smaller than the horizontal, and this difference decreases with age. It is not significantly correlated with refractive errors (Delmarcelle *et al.*, 1976). The depth of the anterior chamber increases from about 3·0 mm at the age of 6 years, to a maximum of 3·25 mm at 15 years and then decreases linearly with age, reaching an average of 2·64 mm at 65 years.

Its inter-individual variations increase with age with a standard deviation of 0·25 mm at 15 years and 0·49 mm at 65 years (Weekers *et al.*, 1973). It presents a variation of 0·05 mm with each diopter of refractive error (Delmarcelle *et al.*, 1976). The thickness of the cornea has an average value of 0·56 mm and a standard deviation of 0·045 mm. It does not vary significantly with age and refraction (Delmarcelle *et al.*, 1976).

There is no significant correlation between the depth of the anterior chamber, the radius of the cornea (Weekers *et al.*, 1961) and the thickness of the cornea (Delmarcelle *et al.*, 1976). Furthermore, their statistical distributions are Gaussian. Therefore the corresponding relative variation of the calibration coefficient can be estimated from eqn. 6, as follows:

$$\left(\frac{\sigma_K}{K}\right)_{global} = \frac{1}{K} \sqrt{\left(\frac{\delta K}{\delta AC}\sigma_{AC}\right)^2 + \left(\frac{\delta K}{\delta AP}\sigma_{DAC}\right)^2 + \left(\frac{\delta K}{\delta AP}\sigma_{TC}\right)^2} \qquad (8)$$

where $\sigma_K$, $\sigma_{AC}$, $\sigma_{DAC}$ and $\sigma_{TC}$ are the standard deviation, respectively, of the calibration coefficient, the radius of the cornea, the depth of the anterior chamber and the thickness of the cornea. The results calculated for age groups of 15 and 65 years are summarised in Table 1. Given that the distribution is Gaussian, the maximum variation of the calibration coefficient for 99% of the population is ±18% for the younger group and ±25% for the older.

As mentioned above, additional information is provided by the measurement of the size of the corneal reflex pattern, allowing the determination of the radius of the cornea. The term that corresponds to the radius of the cornea is eliminated, resulting in the following equation:

$$\left(\frac{\sigma_K}{K}\right)_{compensated} = \frac{1}{K} \sqrt{\left(\frac{\delta K}{\delta AP}\sigma_{DAC}\right)^2 + \left(\frac{\delta K}{\delta AP}\sigma_{TC}\right)^2} \qquad (9)$$

This correction allows a reduction in the variation of the calibration coefficient. This reduction is more important for the younger group (±11%, compared with ±18%) than for the older group (±21%, compared with ±25%), which is the consequence of a much larger variation in the depth of the anterior chamber in the older group.

*Table 1 Average values and standard deviations of parameters of the anterior chamber and corresponding global and compensated calibration coefficients for 15 and 65-year-old subjects*

| | horizontal radius of the cornea, mm | vertical radius of the cornea, mm | depth of the anterior chamber mm | thickness of the cornea, mm | horizontal calibration coefficient $\mu m^{\circ -1}$ | vertical calibration coefficient $\mu m^{\circ -1}$ | compensated calibration coefficient $\mu m^{\circ -1}$ |
|---|---|---|---|---|---|---|---|
| 15 years | 7·95 (0·26) | 7·77 (0·26) | 3·25 (0·25) | 0·56 (0·045) | 81 (6·4) | 79 (6·4) | 80 (4·0) |
| 65 years | 7·69 (0·26) | 7·64 (0·26) | 2·64 (0·49) | 0·56 (0·045) | 86 (9·4) | 86 (9·4) | 86 (7·9) |

*Table 2 Mean quadratic interocular difference between parameters of the anterior chamber and corresponding global and compensated calibration coefficients*

| radius of the cornea, mm | depth of the anterior chamber, mm | calibration coefficient, $\mu m^{\circ -1}$ | compensated calibration coefficient, $\mu m^{\circ -1}$ |
|---|---|---|---|
| 0.07 | 0.12 | 2.0 | 1.9 |

The comparison of the biometry components of the right and left eyes of 100 subjects (BUQUET, 1989*b*) (Table 2) shows that, for 99% of the population, the difference between the calibration coefficient of the right and left eyes is within ±5·7%.

Another important parameter is the angle between the visual and optical axes, which is an offset for the estimations of the gaze direction from the POG measurements. Estimations by different authors of its normal horizontal component present important discrepancies: 5·1°, with variations between 3·5° and 6·0° in emmetropic subjects (DONDERS, 1864); 2·6°, with a standard deviation of 1·7° (FRANCESCHETTI and BURIAN, 1970). This angle is larger for hypermetropic subjects and smaller for myopic subjects. The range of variation in its normal vertical component has not been reported.

### 5.3 Experimental approach

In order to validate these theoretical results and to compensate for the lack of available data, a calibration was performed on a group of 53 subjects with an average age of 45 years. POG measurements were made for five positions of a visual stimulus, one central and four in the four quadrants, at 10° of eccentricity. The calibration coefficients were computed by minimising the mean quadratic error between a first-order linear regression and the measurements obtained for the five fixations. The results, which are summarised in Table 3, are in excellent agreement with the theoretical predictions for the horizontal and vertical calibration coefficients as well as for the horizontal offset. The value of the vertical offset includes the angle between the axis of the optical sensor and the horizontal plane (10°) and the vertical component of the angle between the visual axis and the optical axis of the eye (average value = 1·0°). Its standard deviation is found to be about the same (1·4°) as for the horizontal offset (1·2°).

The horizontal and vertical calibration coefficients present a significant correlation with the size of corneal reflex pattern (Fig. 9). This result confirms the possibility of using this information to identify the radius of the cornea and reduce the inter-individual variability of the calibration coefficients.

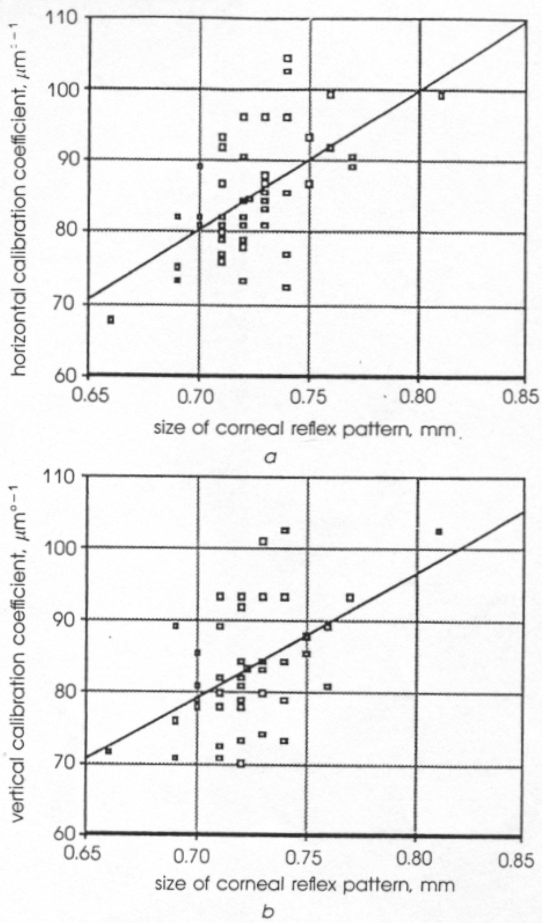


**Fig. 9** *Relationship between calibration factors and the size of the corneal reflex pattern: (a) horizontal component; (b) vertical component*

In the experimental group, the introduction of this correction reduces the variability of the calibration coefficients from ±24% to ±18%. As seen above, the improvement would be more important for a younger population.

## 6 Discussion

The accuracy obtained with different calibration procedures can be estimated from these theoretical and experimental results, assuming that the POG measurements are corrected for the age of the patient and for the size of the corneal reflex pattern.

*Table 3 Average and standard deviation of calibration coefficients obtained during the experimental evaluation*

| | horizontal calibration coefficient, $\mu m^{\circ -1}$ | vertical calibration coefficient, $\mu m^{\circ -1}$ | compensated calibration coefficient, $\mu m^{\circ -1}$ | horizontal offset, ° | vertical offset, ° |
|---|---|---|---|---|---|
| experimental (45 years) | 85 (8·4) | 82 (7·5) | 84 (6·5) | −3·9 (1·2) | 11·0 (1·4) |
| theoretical (15 years) | 81 (6·4) | 79 (6·4) | 80 (4·0) | −5·1 (?) −2·6 (1·7) | ? |
| theoretical (65 years) | 86 (9·4) | 86 (9·4) | 86 (7·9) | −2·6 (1·7) | ? |

If no calibration is used, the maximum offset error for 99% of the population reaches 2·8° horizontally and 3·3° vertically, and the maximum error on the calibration coefficient is 11% for young subjects and 21% for old subjects. The maximum error in the evaluation of dysmetries (inter-ocular comparison of amplitudes) is lower than 6%. A calibration with only one fixation point eliminates the offset error but does not affect the calibration coefficients. Additional points allow the identification of horizontal and vertical calibration coefficients.

## 7 Conclusions

It has been demonstrated that a precise quantification of the static orientations of the eye can be achieved from the measurements of the POG technique. An optical model of the anterior chamber of the eye allows the introduction of correcting factors for the spherical geometry and parallax errors, reducing the mean quadratic error on the estimation of static orientations to 0·5°. This model has been used to study the inter-individual and inter-ocular variability of the calibration factors and to define simplified calibration procedures suitable for clinical applications. It has been shown that additional information, such as the age of the patient and estimation of the corneal curvature radius, can further reduce this variability. Such modelling procedures are helpful when a complete calibration cannot be used, a problem that is often encountered in clinical applications.

*Acknowledgment*—This research was supported by contract DRET N89/244.

## References

AALTO, H., JUHOLA, M., and PYYKKO, I. (1989): 'Visual stimulator using laser beam for eye movement studies,' *Med. & Biol. Eng. & Comput.*, **27**, 3, pp. 332–335

BARBUR, J. L., THOMSON, W. D., and FORSYTH, P. M. (1987): 'A new system for the simultaneous measurement of pupil size and two dimensional eye movements,' *Clin. Vis. Sci.*, **2**, (2), pp. 131–142

BARRY, J. C., EFFERT, R., and KAUPP, A. (1992): 'Objective measurement of small angles of strabismus in infants and children with photographic reflection pattern evaluation,' *Ophthalmol.*, **99**, pp. 320–328

BRODIE, S. E. (1987): 'Photographic calibration of the Hirschberg test,' *Invest. Ophthalmol. Vis. Sci.*, **28**, pp. 736–742

BRONSON, G. W. (1983): 'Potential sources of error when applying a corneal reflex eye-monitoring technique to infant subjects,' *Behav. Methods & Instrum*, **15**, (1), pp. 22–28

BUQUET, C., CHARLIER, J. R., and PARIS, V. (1988): 'Museum application of an eye tracker,' *Med. & Biol. Eng. & Comput.*, **26**, pp. 277–281

BUQUET, C., CHARLIER, J. R., TOUCAS, S., and QUERE, M. A. (1989*a*): 'Comparaison des techniques d'électro-oculographie et de traitement d'images pour l'enregistrement des mouvements oculaires en clinique ophtalmologique,' *Innov. Techn. Biol. Med.*, **10**, (5), pp. 542–552

BUQUET, C. (1989*b*): 'Nouvelle méthode d'évaluation clinique de la statique et de la cinétique oculaire: la photo-oculographie.' Doctorate thesis, University of Lille

CHARLIER, J. R., and HACHE, J. C. (1982): 'New instrument for monitoring eye fixation and pupil size during the visual field examination,' *Med. & Biol. Eng. & Comput.*, **2**, pp. 23–28

CHARLIER, J. R., BARISEAU, J. L., CHUFFART, V., MARSY, F., and HACHE, J. C. (1985): 'Real time pattern recognition and feature analysis from video signals applied to eye movement and pupillary reflex monitoring,' *Doc. Ophthalmol. Proc. Series*, **42**, pp. 181–189

CHARLIER, J. R., and PARIS, V. (1987): 'Model for the determination of the gaze direction from images of the eye.' Proc. European Conf. on Eye Movements, Gottingen, **1**, pp. 9–10

COCHET, P., MARECHAL-COURTOIS, C., and PRIJOT, E. (1976): 'Les verres de contact,' *Bull. Soc. Belge Ophthalmol.*, **145**, pp. 13–52

CRANE, H. D., and STEELE, C. M. (1978): 'Accurate three-dimensional eyetracker,' *Appl. Opt.*, **175**, (5), pp. 691–705

DELMARCELLE, Y., FRANCOIS, J., GOES, F., COLLIGNON-BRACH, J., LUYCKX-BACUS, J., and VERBRAECKEN, H. (1976): 'Biométrie oculaire clinique'. (Masson, Paris)

DONDERS, F. C. (1864): 'On the anomalies of accommodation and refraction of the eye' (The New Sydenham Society, London) (Translated by MOORE, W. D.)

FOURCY, J., PERNIER, J., BEZ, M., and JEANNEROD, M. (1980): 'Cyclope: un capteur de position due globe oculaire non contraignant à base de techniques vidéo et microprocesseur,' *Innov. Technol. Biol. Med.*, **1**, pp. 44–373

FRANCESCHETTI, A. T., and BURIAN, H. M. (1970): 'Proximal convergence. An evaluation by comparison of major amblyoscope and alternate prism and cover test measurement and by AC/A ratio determination.' Strabismus 69 Trans. Consilium Europaeum Strabismi Studio Deditum Congress, Mosby, St Louis, p. 125

GAUTHIER, G. M., and VOLLE, M. (1975): 'Two dimensional eye movement monitor for clinical and laboratory recordings,' *EEG Clin. Neurophysiol.*, **39**, pp. 285–291

HIRSCHBERG, J. (1885): 'Uber die Messung des Schieldgrades und die Dosierung der Schieloperation,' *Zentrabl. Prakt. Augenheild.*, **8**, p. 325

JANTTI, V., AANTAA, E., LANG, H., LAHTI, J., and VIRTANEN, J. (1979): 'Microcomputer-controlled visual stimulator for studies of eye movements and visual evoked potentials,' *Med. & Biol. Eng. & Comput.*, **17**, pp. 881–882

MARG, E. (1951): 'Development of electro-oculography—standing potential of the eye in registration of eye movement,' *AMA Arch. Ophthalmol.*, **45**, pp. 169

MERCHANT, J., MORISSETTE, R., and PORTEFIELD, J. L. (1974): 'Remote measurement of eye direction allowing subject motion over one cubic foot of space,' *IEEE Trans.*, **BME-21**, pp. 309–317

QUERE, M. A., FRETTAY, C. LE BORGNE, R., DELPLACE, M. P., and DEVLAMYNCK, S. (1972): 'L'exploration multiparamétrique de la cinétique oculaire,' *Ann. d'Oculist. (Paris)*, **205**, pp. 1307–1320

QUERE, M. A., DEVLAMINCK, S., DELPLACE, M. P., and LE BORGNE, R. (1973): 'La répartition physiologique des potentiels électro-oculographiques: le champ périoculaire: préliminaires,' *Rev. Oto. Neuro. Ophtalmol.*, **34-2**, pp. 135–138

QUERE, M. A., TOUCAS, S., BUQUET, C., CHARLIER, J. R., LAVENANT, F., and PECHEREAU, A. (1990*a*): 'Photo-oculographie différentielle des mouvements verticaux et obliques,' *Ophtalmologie*, **4**, pp. 109–115

QUERE, M. A., TOUCAS, S., BUQUET, C., and CHARLIER, J. R. (1990*b*): 'La cinétique des insuffisances de convergence. Etude électro-oculographique et photo-oculographique,' *Bull. Soc. Ophalmol. Fr.*, **11**, pp. 1079–1087

QUERE, M. A., TOUCAS, S., BUQUET, C., and CHARLIER, J. R. (1990*c*): 'Analyse des mouvements de vergence par photo-oculographie différentielle,' *Ophtalmologie*, **4**, pp. 270–274

REINECKE, R. D. (1961*a*): 'Selected studies with electro-oculograms I-Report of disjunctive eye movements recorded on electro-oculograms,' *Arch. Ophthalmol.*, **66**, pp. 125–129

REINECKE, R. D. (1961*b*): 'Selected studies with electro-oculograms II-Subjective evaluation of ocular proprioception monitored with the use of electro-oculograms,' *Ibid.*, **66**, pp. 130–132

REULEN, J. P. H., MARCUS, J. T., KOOPS, D., DEVRIES, F. R., TIESINGA, G., and BOSHUIZEN, K. (1988): 'Precise recording of eye movements: the iris technique,' *Med. & Biol. Eng. & Comput.*, **26**, pp. 20–32

ROBINSON, D. A. (1963): 'A method of measuring eye movements using a search coil technique in a magnetic field,' *IEEE Trans.*, **BME-10**, pp. 137–145

SMITH, W. M., and WARTER, P. J. (1960): 'Eye movement and stimulus movement: new photoelectric electromechanical system for recording and measuring tracking motions of the eye,' *J. Opt. Soc. Am.*, **50**, p. 245

T[illegible], N., GUILLEMIN, V. and BARTHONY, J. M. (1951): 'Photo-electro-nystagmography.' Ann. Oto. Rhinol. Laryngol., **60**, p. 917
WEEKERS, R., GRIETEN, J. and LAVERGNE, G. (1961): 'Etude des dimensions de la chambre antérieure de l'oeil humain. I-Considérations biometriques.' *Ophthalmologica (Basel)*, **142**, pp. 650–652
WEEKERS, R., DELMARCELLE, Y., COLLIGNON-BRACH, C., and LUYCKX, J. (1973): 'Mesure optique de la profondeur de la chambre anterieure.' *Doc. Ophthalmol.*, **34**, pp. 413–434
YOUNG, L. R., and SHEENA, D. (1975): 'Survey of eye movement recording methods.' *Behav. Res. Methods & Instrum.*, **7**, pp. 397–429
ZAO, Z. Z., GERBIN, J., and REMOND, A. (1952): 'Le champ électrique de l'oeil.' *Sem. Hôp. Paris*, **28**, pp. 1506–1513

## Appendix

*Young's paraxial equations*

$$\frac{n' \cos^2 \Theta'}{IT'} - \frac{n \cos^2 \Theta}{IT} = \frac{n' \cos \Theta' - n \cos \Theta}{R_y}$$

ANNEX I
PARAXIAL EQUATIONS OF YOUNG

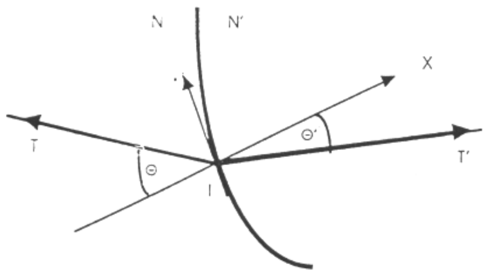


Fig. 10

where *xyz* is a tridimensional referential; *T'* is the virtual image of *T* through the optical diopter; *n* and *n'* are the indices of the two optical media separated by the diopter; and $R_y$ is the curvature radius in point *I* (Fig. 10).

## Authors' biographies

Cathy Buquet was born in France in 1963. She graduated from the Institut Supérieur d'Electronique du Nord in 1985 and received her Doctorate from Lille University in 1989. Her research interests are in the evaluation of visual functions in children and the evaluation of eye-movement disorders in ophthalmology and neurology.

Jacques Charlier was born in France in 1951. He graduated from the Ecole Centrale de Lyon in 1974, received his MSc in Bio-engineering from the Pennsylvania State University in 1976 and his Doctorate from Lille University in 1979. He is currently a Researcher at the National Institute of Health & Medical Research and a Consultant to the Metrovision company in Villeneuve d'Ascq (France). His research interests are mainly the evaluation of visual functions in humans, including visual field, visual electrophysiology and eye movements.